

## Medicinal Chemistry &amp; Drug Discovery

# Synthesis of 1,2,3-Triazolo-fused-tetrahydro- $\beta$ -carboline Derivatives via 1,3-Dipolar Cycloaddition Reaction: Cytotoxicity Evaluation and DNA-Binding studies

Shalini Nekkanti,<sup>[a]</sup> Venkatesh Pooladanda,<sup>[b]</sup> Mamatha Veldandi,<sup>[a]</sup> Ramya Tokala,<sup>[a]</sup> Chandraiah Godugu,\*<sup>[b]</sup> and Nagula Shankaraiah\*<sup>[a]</sup>

A diverse array of polyheterocyclic annulated 1,2,3-triazolo-fused-tetrahydro- $\beta$ -carboline derivatives have been synthesized via an intramolecular azide-alkyne cycloaddition (1,3-dipolar) reaction. Among the hexaheterocyclic series **5a–r**, the compound **5b** (14,15-dimethoxy-6,7,12,12b-tetrahydro-4H-benzo[5',6'][1,2,3]triazolo[5'',1'':3',4'][1,4]diazepino[1',7':1,2]pyrido[3,4-b]indole) displayed significant cytotoxicity against the MCF-7 cell line with an IC<sub>50</sub> value of 6.45 ± 0.37  $\mu$ M; whereas, among the pentaheterocyclic series **14a–l**, the derivative **14b** ((6*R*,12a*S*)-6-(3,4-dimethoxyphenyl)-7,12,12a,13-tetrahydro-4*H*,6*H*-[1,2,3]triazolo[1'',5'':4',5']pyrazino[1',2':1,6]pyrido[3,4-b]indole) has shown potent cytotoxicity with an IC<sub>50</sub> value of 4.01 ± 0.39  $\mu$ M on the B16F10 cell line. Treatment of MCF-7 and B16F10 cells with **5b** and **14b** respectively resulted in cell cycle arrest, inhibition of cell migration and colony formation as well as induction of apoptosis. DNA binding affinity estimation by viscometry experiment and molecular modeling revealed their efficient minor groove binding.

## Introduction

Indole-based annulated polyheterocycles are structurally diverse frameworks arising from an indole moiety fused to varied privileged heterocycles.<sup>[1]</sup> Due to the wide range of biological activities<sup>[2]</sup> associated with these scaffolds, they offer an inspiration for designing promising leads against various diseases. The  $\beta$ -carboline scaffold, an indole heterocyclic, occurs endogenously in plants and marine organisms with great structural diversity.<sup>[3]</sup> In this class of heterocycles, tetrahydro- $\beta$ -carboline (TH $\beta$ C, Figure 1a) based compounds of natural and synthetic origin possess a broad spectrum of pharmacological activities including potent antitumor activity.<sup>[4]</sup> They exhibit their antitumor activity mainly through multiple mechanisms, such as interaction with DNA,<sup>[5]</sup> inhibiting topoisomerase II,<sup>[6]</sup> phosphodiesterase 5 (PDE5),<sup>[7]</sup> Transforming Growth Factor-beta (TGF- $\beta$ ),<sup>[8]</sup> Cyclin-Dependant Kinases (CDK)<sup>[9]</sup> and mitotic kinesin Eg5.<sup>[10]</sup> Eudistomin K (**b**),<sup>[11]</sup> Evodiamine (**c**),<sup>[12]</sup> and Azatoxin (**d**)<sup>[13]</sup> are some of the natural polyheterocyclic annulated TH $\beta$ Cs that display potent cytotoxic activities against various cancer cell lines. Recently, there has been growing

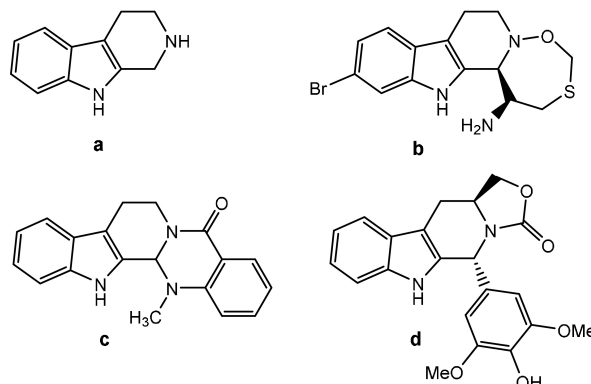


Figure 1. Tetrahydro- $\beta$ -carboline (**a**) and natural cytotoxic compounds (**b**, **c** and **d**) containing the tetrahydro- $\beta$ -carboline scaffold.

interest in developing antitumor compounds based on this scaffold.<sup>[14]</sup>

On the other hand, several molecules possessing 1,2,3-triazole scaffold have been synthesized as useful chemotherapeutic agents with diverse pharmacological activities.<sup>[15]</sup> This is due to the ability of triazole to readily associate with biological targets such as DNA through hydrogen-bonding and other non-covalent interactions, its metabolic stability, and also improved solubility.<sup>[16]</sup> The intermolecular azide-alkyne 1,3-dipolar cycloaddition reaction has remained as one of the classical methods for the synthesis of 1,2,3-triazoles with widespread applications in chemistry and biology.<sup>[17]</sup> In addition to this, the intramolecular azide-alkyne cycloaddition strategy finds application in the synthesis of triazole linked polypeptides and triazole-annulated polyheterocycles.<sup>[18]</sup> This intramolecular

[a] S. Nekkanti, M. Veldandi, R. Tokala, Dr. N. Shankaraiah

Department of Medicinal Chemistry  
National Institute of Pharmaceutical Education and Research (NIPER)  
Hyderabad 500 037, India  
E-mail: shankar@niperhyd.ac.in

[b] V. Pooladanda, Dr. C. Godugu

Department of Regulatory Toxicology  
National Institute of Pharmaceutical Education and Research (NIPER)  
Hyderabad 500 037, India  
E-mail: chandra.niperhyd@gov.in

Supporting information for this article is available on the WWW under <https://doi.org/10.1002/slct.201700620>

reaction can furnish multiple annulated cyclic ring systems in a single step and can thus be considered as a useful strategy for the rapid generation of molecular complexity.

Traditional anticancer drugs usually possess only slight specificity and are often toxic to normal tissues. So, there is a need to design sequence-selective anticancer drugs, such as those that bind to a specific region of DNA involved in the transcription and replication processes. DNA minor groove binders represent a class of anticancer agents whose DNA sequence specificity may lead to a high selectivity.<sup>[19]</sup> Their binding is specific to thymine–adenine (TA) sequences through a combination of hydrogen-bonding, van der Waals contacts, and electrostatic interactions.<sup>[20]</sup> Recently, some new DNA minor groove binders have shown good antitumor activity in preclinical tests and have therefore been selected for clinical investigation.<sup>[21]</sup> Rational structural modifications of these bioactive scaffolds may result in the development of novel leads with better DNA binding affinity.

In view of the biological importance and DNA binding propensity of both 1,2,3-triazole and tetrahydro- $\beta$ -carboline, it was of considerable interest to develop new derivatives incorporating both the frameworks through molecular hybridization (Figure 2). Such a combination could potentially amplify

dro- $\beta$ -carboline derivatives via intramolecular 1,3-dipolar cycloaddition reaction. These new hybrid molecules comprising of two pharmacophoric groups i.e., a tetrahydro- $\beta$ -carboline ring and the annulated 1,2,3-triazole moiety were also explored for their cytotoxicity and DNA-binding affinity.

## Results and Discussion

### Chemistry

The strategy followed for the synthesis of 1,2,3-triazolo-fused-tetrahydro- $\beta$ -carboline derivatives is depicted in Scheme 1 and 2. In Scheme 1, the nitro group of 2-nitro benzaldehyde (**1a**) and 6-nitroveratraldehyde (**1b**) was directly converted into azide by nucleophilic substitution with sodium azide in HMPA at 20 °C.<sup>[23]</sup> Next, the *o*-azidobenzaldehydes **2a,b** were allowed to undergo Pictet-Spengler cyclization with tryptamine under acidic conditions to yield the tetrahydro- $\beta$ -carbolines **3a,b**. Subsequently, the secondary nitrogen of ring C is propargylated by using propargyl bromide and potassium carbonate under a nitrogen atmosphere to yield the azido-alkynes **4a,b** in quantitative yields. The crucial step involves the intramolecular azide-alkyne 1,3-dipolar cycloaddition by refluxing the crude azido-alkynes in toluene until TLC indicated the completion of the reaction, to yield the hexaheterocyclic annulated system **5a,b**. Structurally diverse analogues of the hexaheterocyclic ring system, **5c–r** were synthesized in excellent yields by indole N-alkylation with diverse halides in the presence of NaH.

In Scheme 2, the tetrahydro- $\beta$ -carbolines **9a–l** were obtained via Pictet-Spengler cyclization of the methyl ester of L-tryptophan (**7**) with diversely substituted benzaldehydes **8a–f** under acidic conditions. The two diastereomers (*cis* and *trans*) so obtained were separated by column chromatography and then characterized. In each of the diastereomer, the ester functionality was selectively reduced to the corresponding alcohols **10a–l** by LiAlH<sub>4</sub>, followed by tosylation and further conversion to its azides **12a–l** using sodium azide. The respective key intermediates i.e., the azido-alkynes **13a–l** were synthesized by propargylation of the secondary nitrogen of ring C using propargyl bromide and potassium carbonate under a nitrogen atmosphere. The final step involves the intramolecular azide-alkyne 1,3-dipolar cycloaddition by refluxing the crude azido-alkynes **13a–l** in toluene until TLC indicated completion of the reaction, to yield the pentaheterocyclic annulated systems **14a–l** in overall good yields.

In particular, our strategy involved the catalyst-free intramolecular 1,3-dipolar cycloaddition to yield diverse 1,5-disubstituted polyheterocyclic annulated 1,2,3-triazolo-fused-tetrahydro- $\beta$ -carbolines in good to excellent yields. In this protocol, the tailor-made tetrahydro- $\beta$ -carboline-derived azido-alkyne intermediates possessing both alkyne and azide moieties in the same molecule undergo intramolecular Huisgen 1,3-dipolar cycloaddition. Therefore, without further purification, the crude reaction mixture of azido-alkynes was subjected to thermal cycloaddition (toluene, 110 °C, 0.5–1 h) to afford the hexaheterocyclic and pentaheterocyclic annulated 1,2,3-triazolo-fused-tetrahydro- $\beta$ -carbolines as title compounds **5a–r** and **14a–l**.

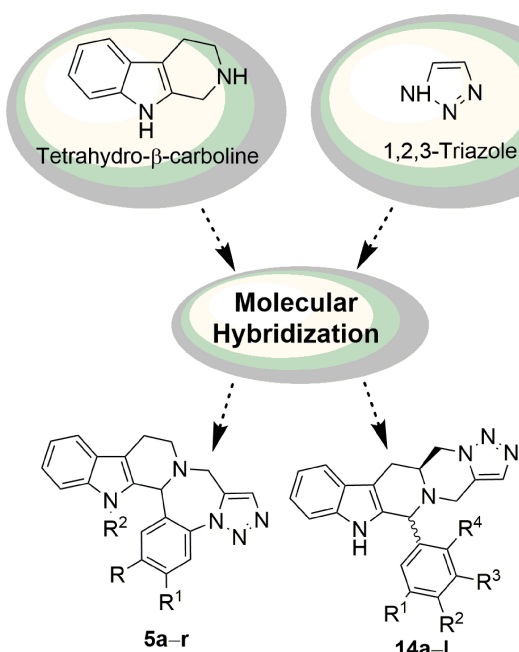
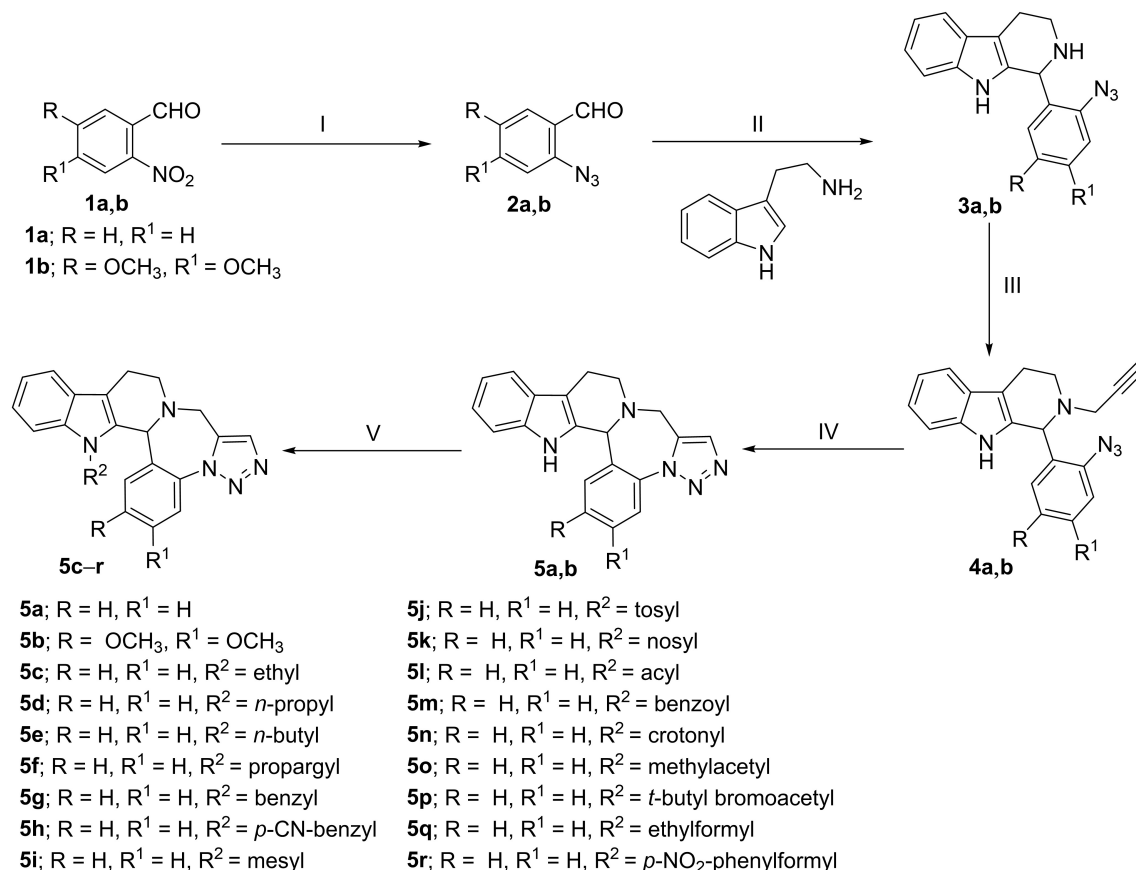


**Figure 2.** Molecular hybridization strategy for the design of 1,2,3-triazolo-fused-tetrahydro- $\beta$ -carboline derivatives as DNA-minor groove binding agents.

the DNA interaction by retaining essential binding features of the parent scaffolds through synergism. Thus, in continuation of our previous research in the arena of anti-cancer  $\beta$ -carbolines and their novel synthetic strategies,<sup>[22]</sup> we have designed and synthesized two diverse series of 1,2,3-triazolo-fused-tetrahy-



**Scheme 1.** Synthesis of hexaheterocyclic annulated 1,2,3-triazolo-fused-tetrahydro-β-carboline derivatives **5a–r**. Reagents and conditions: (I)  $\text{NaN}_3$ , HMPA, 20 °C, 12–14 h, 95% (**2a**), 89% (**2b**); (II) 5% TFA/CH<sub>2</sub>Cl<sub>2</sub>, 0 °C to rt, 18–24 h, 96% (**3a**), 91% (**3b**); (III)  $\text{K}_2\text{CO}_3$ , propargyl bromide, DMF, 0 °C to rt, 3–4 h, 98% (**4a**), 97% (**4b**); (IV) toluene, reflux, 0.5–1 h, 96% (**5a**), 90% (**5b**); (V)  $\text{NaH}$ ,  $\text{R}'\text{X}$ , DMF, 0 °C to rt, 2–4 h, 90–97%.

respectively. As shown in Scheme 1, there was a wide tolerance for diverse indole N-substitutions on the tetrahydro-β-carboline core. Gratifyingly, tetrahydro-β-carbolines with both electron-rich and electron-poor substituents on the C6 phenyl ring underwent the desired reaction in good yields as shown in Scheme 2. Finally, the compounds **5a–r** and **14a–l** were unambiguously characterized by HRMS (ESI), <sup>1</sup>H and <sup>13</sup>C NMR spectroscopic techniques.

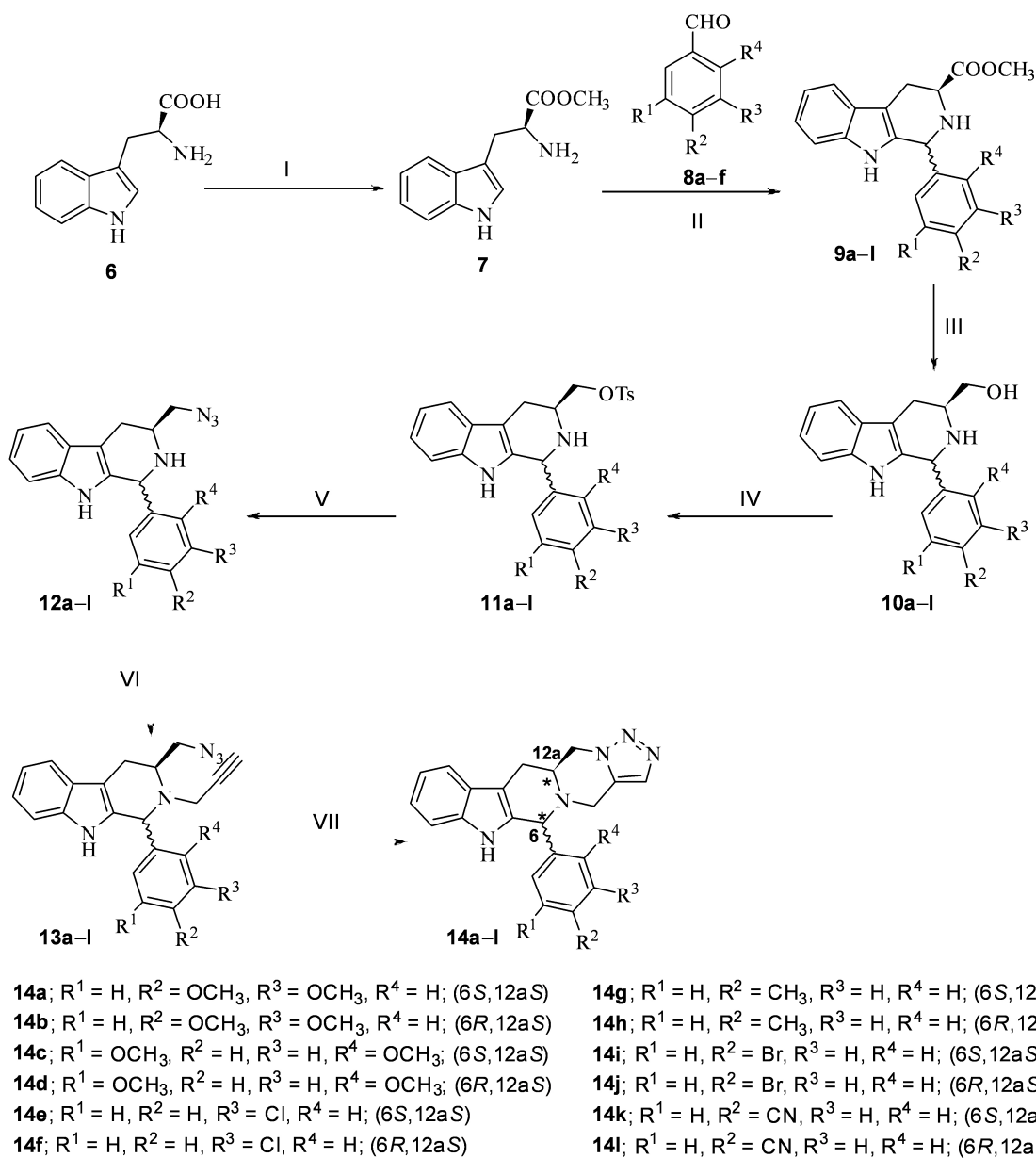
The <sup>1</sup>H NMR spectrum of **5a** showed a sharp singlet at  $\delta$  7.77 in the aromatic region, typical for the 1,2,3-triazole hydrogen. Similar singlets were observed in the aromatic region ( $\delta$  7.75–7.90) of <sup>1</sup>H NMR spectra of **5b–r**. The indole NH proton in **5a** and **5b** appears as broad singlets at  $\delta$  8.26 and 8.33 respectively, whereas they are absent in the N-alkylated compounds **5c–r**. In the pentaheterocyclic series **14a–l**, the <sup>1</sup>H and <sup>13</sup>C NMR spectra for the *cis*-(6*S*,12*aS*) and *trans*-(6*R*,12*aS*) diastereomers were almost similar except for the peak corresponding to the C6 stereocenter in <sup>13</sup>C NMR; in the *trans*-diastereomers, it exhibited comparatively up-field (~4–5 ppm) chemical shifts.<sup>[24]</sup> For instance, in **14a** (*cis*-) and **14b** (*trans*), the peaks corresponding to the C6 appear at 64.5 and 60.3 ppm, respectively. The HRMS (ESI) of all the compounds

displayed the characteristic  $[\text{M} + \text{H}]^+$  peaks corresponding to their molecular formula.

#### In vitro cytotoxic activity

The newly synthesized 1,2,3-triazolo-fused-tetrahydro-β-carboline derivatives **5a–r** and **14a–l** were screened for their in vitro cytotoxicity against selected cancer cell lines *viz.* human lung (A549), breast (MDA-MB-231 and MCF-7), liver (SK-HEP-1) along with mouse melanoma (B16F10) and normal rat as well as human fibroblasts (NRK-49F and HFL-1, respectively) using 3-(4,5-dimethylthiazol-2-yl)-2,5-diphenyltetrazolium bromide (MTT) assay. Harmine, a natural cytotoxic β-carboline alkaloid was used as the reference standard and the  $\text{IC}_{50}$  ( $\mu\text{M}$ ) values (concentration required to inhibit 50% of cancer cells growth) of the tested compounds were listed in Table 1.

It was apparent from the initial screening results that some of the synthesized compounds possessed moderate to potent growth inhibition against the tested cancer cell lines. Among the series **5a–r**, the compound **5b** displayed significant cytotoxicity with  $\text{IC}_{50}$  values of  $8.50 \pm 0.84$ ,  $9.02 \pm 1.77$  and  $6.45 \pm 0.37 \mu\text{M}$  on A549, MDA-MB-231, and MCF-7 cell lines,



**Scheme 2.** Synthesis of pentaheterocyclic annulated 1,2,3-triazolo-fused-tetrahydro- $\beta$ -caroline derivatives **14a–l**. Reagents and conditions: (I)  $\text{SOCl}_2$ ,  $\text{MeOH}$ ,  $0^\circ\text{C}$  to rt, 4 h, 98%; (II) 5%  $\text{TFA}/\text{CH}_2\text{Cl}_2$ ,  $0^\circ\text{C}$  to rt, 18–24 h, 90–96%; (III)  $\text{LiAlH}_4$ ,  $\text{THF}$ ,  $0^\circ\text{C}$  to rt, 4 h, 96%; (IV)  $\text{TsCl}$ ,  $\text{DMAP}$ ,  $\text{Et}_3\text{N}$ ,  $\text{CH}_2\text{Cl}_2$ ,  $0^\circ\text{C}$  to rt, 12 h, 90–92%; (V)  $\text{NaN}_3$ ,  $\text{DMF}$ ,  $60^\circ\text{C}$ , 6–8 h, 92–96%; (VI)  $\text{K}_2\text{CO}_3$ , propargyl bromide,  $\text{DMF}$ ,  $0^\circ\text{C}$  to rt, 3–4 h, 96–98%; (VII) toluene, reflux, 0.5–1 h, 75–87%.

respectively. The compound **5a** appears to be selectively cytotoxic towards the SK-HEP-1 cell line with an  $\text{IC}_{50}$  of  $24.99 \pm 3.96 \mu\text{M}$ , while the compounds **5b**, **5j**, **5k**, and **5m** have displayed moderate cytotoxicities compared to Harmine ( $24.16 \pm 2.82 \mu\text{M}$ ), with  $\text{IC}_{50}$  values ranging from  $29.14 \pm 5.12$  to  $29.85 \pm 5.14 \mu\text{M}$ . Most of the compounds displayed moderate cytotoxicities in the range from 25 to 49  $\mu\text{M}$  on the cell lines investigated while the rest of the compounds were found to be inactive ( $\text{IC}_{50} > 50 \mu\text{M}$ ).

Among the series **14a–l**, the compound **14b** was the most potent with significant  $\text{IC}_{50}$  values of  $18.36 \pm 1.39$ ,  $4.01 \pm 0.39$  and  $10.82 \pm 1.03 \mu\text{M}$  on A549, B16F10 and SK-HEP-1 cell lines respectively. On the A549 cell line, **14b**, **14d** and **14j** have displayed  $\text{IC}_{50}$  values in the range from  $18.36 \pm 1.39$  to  $19.50 \pm 3.09 \mu\text{M}$ , comparable to that of Harmine ( $18.26 \pm 1.71 \mu\text{M}$ ). Moreover, compounds **14b**, **14d**, **14h** and **14j** ( $4.01 \pm 0.39$ ,  $4.87 \pm 0.46$ ,  $5.61 \pm 0.88$  and  $10.82 \pm 4.74 \mu\text{M}$ , respectively) have displayed significantly higher cytotoxicity than Harmine ( $18.12 \pm 1.65 \mu\text{M}$ ) against the B16F10 cell line. On the MDA-

**Table 1.** IC<sub>50</sub> ( $\mu$ M) values<sup>[a]</sup> for the derivatives 5a–r and 14a–l by MTT assay

Compounds	A549[b]	B16F10[c]	MDA-MB-231[d]	MCF-7[e]	SK-HEP-1[f]	NRK-49F[g]	HFL-1[h]
5a	28.26 ± 8.14	38.16 ± 3.12	>50	30.65 ± 4.18	24.99 ± 3.96	-	-
5b	8.50 ± 0.84	23.18 ± 2.28	9.02 ± 1.77	6.45 ± 0.37	29.14 ± 5.12	22.02 ± 3.47	24.55 ± 2.03
5c	49.08 ± 6.17	39.11 ± 1.16	29.99 ± 8.14	>50	50.16 ± 8.21	-	-
5d	30.48 ± 5.16	39.01 ± 7.41	29.51 ± 5.12	35.14 ± 1.56	>50	-	-
5e	40.83 ± 7.84	31.09 ± 6.19	29.17 ± 1.02	48.58 ± 3.24	39.61 ± 1.59	-	-
5f	>50	29.26 ± 8.25	32.17 ± 2.89	49 ± 2.13	>50	-	-
5g	49.01 ± 1.23	35.21 ± 5.87	27.15 ± 2.69	30.10 ± 2.19	47.23 ± 5.84	-	-
5h	31.71 ± 0.55	29.86 ± 2.10	>50	25.05 ± 2.29	>50	-	-
5i	32.79 ± 0.85	30.19 ± 0.98	50.20 ± 2.10	30.14 ± 4.71	31.25 ± 2.54	-	-
5j	>50	28.56 ± 1.91	29.15 ± 5.59	>50	29.56 ± 1.28	-	-
5k	49.98 ± 2.23	50.09 ± 8.14	48.21 ± 1.23	42.79 ± 1.59	29.85 ± 5.14	-	-
5l	>50	29.56 ± 1.26	41.09 ± 1.01	46.18 ± 5.29	31.25 ± 6.02	-	-
5m	30.15 ± 7.18	40.19 ± 4.39	37.02 ± 3.96	32.87 ± 1.26	29.84 ± 1.05	-	-
5n	42.17 ± 1.89	39.56 ± 4.10	>50	46.98 ± 1.45	30.19 ± 0.17	-	-
5o	36.15 ± 9.01	28.25 ± 0.11	36.12 ± 2.69	46.28 ± 2.98	>50	-	-
5p	30.12 ± 4.15	>50	29.63 ± 2.13	47.16 ± 1.19	>50	-	-
5q	36.17 ± 4.56	50.12 ± 9.12	31.25 ± 6.10	30.12 ± 2.47	50.61 ± 2.12	-	-
5r	33.83 ± 2.47	29.31 ± 0.12	>50	49.08 ± 0.98	>50	-	-
14a	36.16 ± 2.51	42.19 ± 3.10	31.30 ± 1.10	30.12 ± 2.40	38.67 ± 2.02	-	-
14b	18.36 ± 1.39	4.01 ± 0.39	22.76 ± 0.98	14.12 ± 7.62	10.82 ± 1.03	30.84 ± 2.29	18.18 ± 0.95
14c	36.17 ± 4.52	>50	30.21 ± 6.15	>50	>50	-	-
14d	18.71 ± 2.61	4.87 ± 0.46	>50	31.20 ± 0.19	29.56 ± 2.18	-	-
14e	31.10 ± 1.46	42.11 ± 2.24	33.12 ± 2.23	29.56 ± 5.11	45.61 ± 2.02	-	-
14f	33.83 ± 2.47	29.30 ± 0.11	>50	>50	>50	-	-
14g	>50	39.11 ± 1.16	29.99 ± 8.14	>50	>50	-	-
14h	21.50 ± 0.12	5.61 ± 0.88	5.82 ± 0.24	29.61 ± 2.01	28.26 ± 5.69	-	-
14i	29.17 ± 4.16	45.01 ± 3.12	31.25 ± 6.12	31.13 ± 1.37	>50	-	-
14j	19.50 ± 3.09	10.82 ± 4.74	29.56 ± 5.12	>50	30.56 ± 5.12	-	-
14k	28.14 ± 0.50	>50	28.25 ± 2.11	29.06 ± 0.12	>50	-	-
14l	30.10 ± 0.90	>50	29.16 ± 0.14	30.10 ± 2.47	>50	-	-
Harmine	18.26 ± 1.71	18.12 ± 1.65	14.14 ± 1.82	4.69 ± 0.92	24.16 ± 2.82	-	-

[a] 50% Inhibitory concentration after 48 h of drug treatment. [b] Human lung cancer. [c] Mouse melanoma. [d] [e] Human breast cancer. [f] Human liver cancer. [g] Rat fibroblast. [h] Human lung fibroblast.

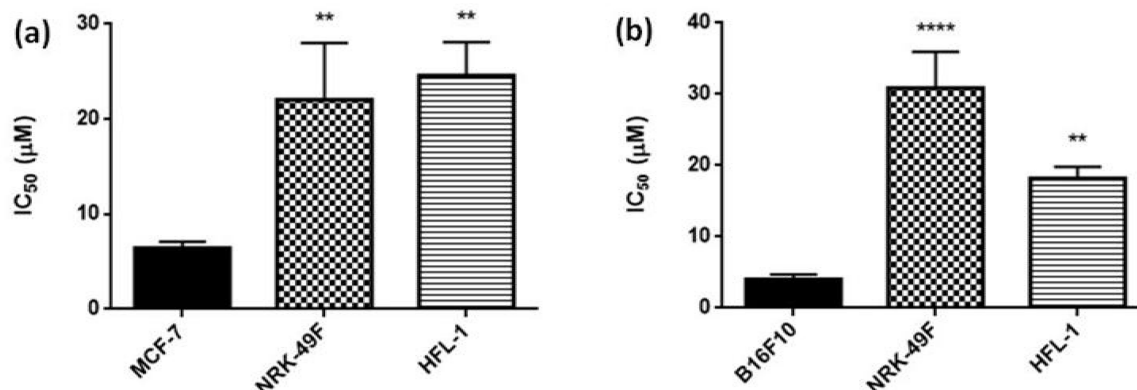


**Figure 3.** Cytospecificity of (a) 5b and (b) 14b towards cancer cells (MCF-7 and B16F10, respectively) compared to normal fibroblasts (NRK-49F and HFL-1). The values were expressed as mean ± S.E.M. (n=3) \*\*p<0.01 and \*\*\*\*p<0.0001 versus cancer cell lines MCF-7 and B16F10.

MB-231 cell line, only the compound 14h (5.82 ± 0.24  $\mu$ M) was found to be more potent than Harmine (14.14 ± 1.82  $\mu$ M). On the other hand, none of the compounds tested were more active than Harmine against the MCF-7 cell line.

From the results of Table 1, it was apparent that two compounds viz. 5b and 14b have shown the best in vitro

cytotoxic activity against the breast cancer (MCF-7) and melanoma (B16F10) cell lines, respectively. In order to find out their specificity toward cancer cells, they were further tested for in vitro cytotoxicity on normal renal fibroblast (NRK-49F) and lung fibroblast (HFL-1) cell lines and the results were shown in Figure 3. It was quite interesting to observe that compound 5b

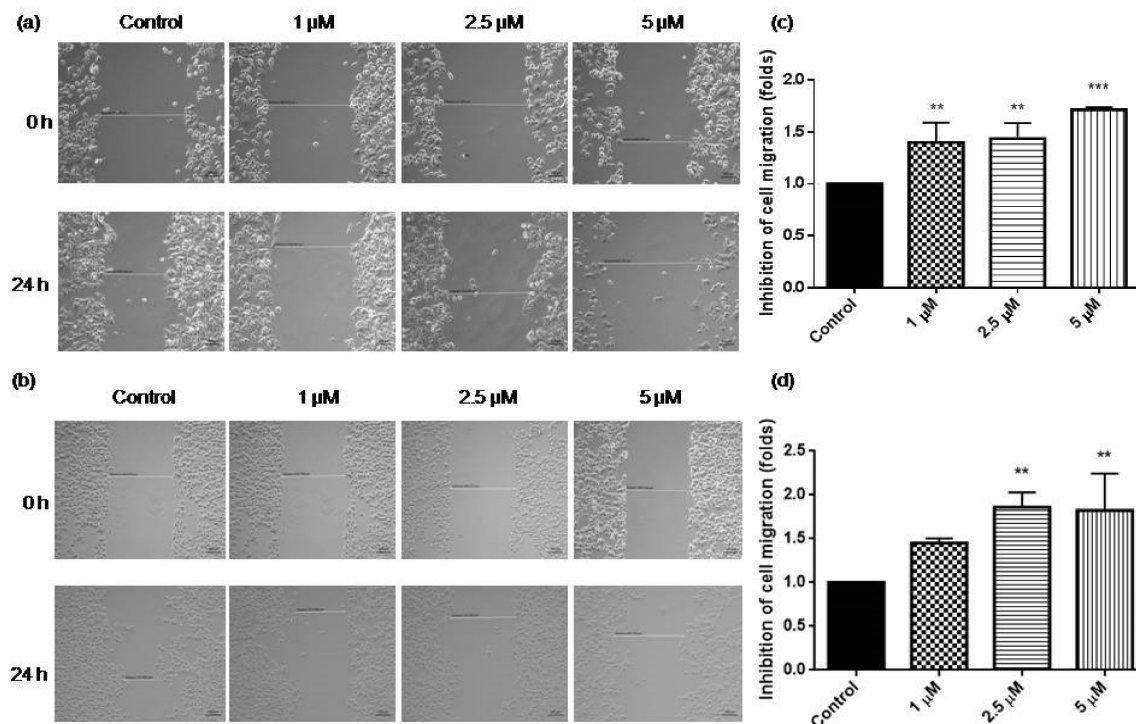


**Figure 4.** In vitro cell migration assay. (a) MCF-7 cells were treated with the compound **5b** (1, 2.5 and 5  $\mu$ M). (b) B16F10 cells were treated with the compound **14b** (1, 2.5 and 5  $\mu$ M). Artificial scratches were done with a sterile 200  $\mu$ L pipette and the images were captured by using phase contrast microscopy at 0 and 24 h. (c) and (d) the relative inhibition of cell migration (folds) of MCF-7 and B16F10 cells upon **5b** and **14b** treatment, respectively after 24 h, quantified using Carl Zeiss Zen software. Data presented were mean  $\pm$  S.E.M of three similar independent experiments, \*\* $p$  < 0.01 and \*\*\* $p$  < 0.001 versus control at 24 h.

has shown highly selective cytotoxicity towards the MCF-7 cell line with an  $IC_{50}$  value of  $6.45 \pm 0.37 \mu$ M as compared to normal fibroblast cell lines, NRK-49F and HFL-1 ( $IC_{50}$  values of  $22.02 \pm 3.47$  and  $24.55 \pm 2.03 \mu$ M, respectively). The compound **14b** has shown more cytotoxicity towards the B16F10 cell line with an  $IC_{50}$  value of  $4.01 \pm 0.39 \mu$ M compared to NRK-49F and HFL-1 ( $IC_{50}$  values of  $30.84 \pm 2.29 \mu$ M and  $18.18 \pm 0.95 \mu$ M, respectively). Thus, the compound **5b** displayed almost 3 and 4 fold more selectivity towards MCF-7 cell line when compared to NRK-49F and HFL-1 cells, respectively; whereas, the compound **14b** was 8 and 4 fold more selective towards the B16F10 cell line than NRK-49F and HFL-1 cells, respectively. As **5b** and **14b** have shown promising and selective cytotoxicity towards cancer cells, we were encouraged to study their mechanism of cell growth inhibition at the cellular level.

#### In vitro cell migration/wound healing assay

As cell migration and motility are associated with the metastatic activity of cancer cells,<sup>[25]</sup> we have investigated the effect of compounds **5b** and **14b** on MCF-7 and B16F10 cells, respectively, using the wound healing assay. This assay is based on the principle that, upon making an artificial wound on a confluent cell monolayer, the cells on the edge of the wound will migrate inwards to close it. This migration of cells to close

the wound is restricted by the treatment with an anticancer agent. Wounds were created on a confluent cell monolayer culture of MCF-7 and B16F10 cells by using a sterile 200  $\mu$ L pipette tip and then treated with 1, 2.5 and 5  $\mu$ M of the compounds. The migration of MCF-7 and B16F10 cells was recorded by microscopic observations at 0 h and 24 h.

From Figure 4a, it can be clearly observed that there was a healing of the wound in the untreated control cells after 24 h, however, healing was strongly suppressed in the MCF-7 cells treated with **5b**. Quantification of the results has shown 1.39 and 1.43 fold (at 1 and 2.5  $\mu$ M, respectively) decrease in migration of MCF-7 cells in relative comparison to vehicle treated control cells. The effect was more prominent with 5  $\mu$ M, wherein a 1.71 fold inhibition of cell migration after 24 h was observed. As seen in Figure 4b, a complete healing of the wound in control cells after 24 h and strong inhibition by **14b** in B16F10 cells, was observed. Quantified results have revealed that there were 1.45 and 1.85 fold decreased migrations of B16F10 cells with 1 and 2.5  $\mu$ M concentrations, respectively in relative comparison to control cells. There was a comparable effect with 5  $\mu$ M concentration, wherein 1.82 fold decreased cell migration was observed after 24 h. These results definitely indicate that the migration of MCF-7 and B16F10 cancer cells was substantially suppressed by the 1,2,3-triazolo-fused-tetrahydro- $\beta$ -carboline derivatives **5b** and **14b**, respectively.

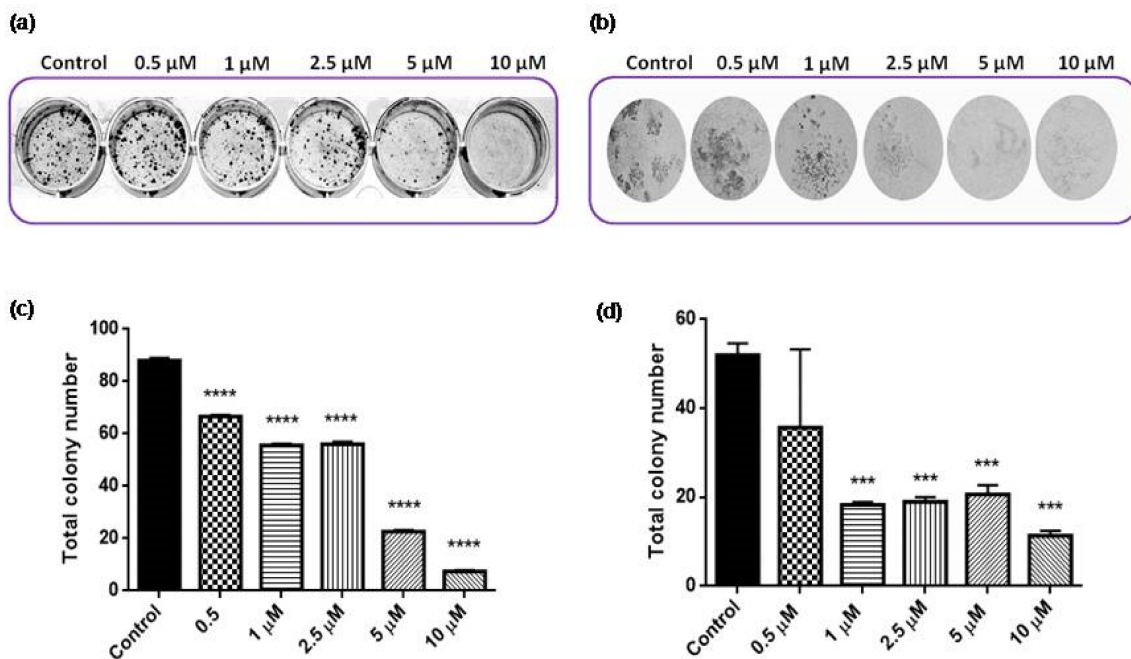


**Figure 5.** Effect of the compounds (a) **5b** and (b) **14b** on the clonogenic growth of MCF-7 and B16F10 cells, respectively. (c) and (d) total colonies of MCF-7 and B16F10 at increasing concentrations of **5b** and **14b**, respectively. They were counted automatically by Vilber Fusion Fx software and the data were quantified by GraphPad Prism 6.01. The values were expressed as mean  $\pm$  S.E.M of three similar independent experiments, \*\*\* $p < 0.001$  and \*\*\*\* $p < 0.0001$  versus control.

### Clonogenic growth inhibition assay

Antiproliferative activity of the most potent compounds **5b** and **14b** were further established by the clonogenic cell growth inhibition assay which conveys the ability of a single cell to grow into a colony and also predicts the response of an individual patient's tumor.<sup>[26]</sup> As observed in Figure 5a, the compound **5b** could effectively inhibit the clonogenic growth of MCF-7 cells at 0.5 μM, the lowest tested concentration. At a concentration of 10 μM, the colony formation was completely inhibited by the compound **5b** which indicated its ability of dose dependent inhibition of colony formation and proliferation of MCF-7 cells. On the other hand, results from Figure 5b showed that compound **14b** dramatically inhibited the clonogenic growth in the B16F10 cell line at the lowest concentration of 0.5 μM, similar to **5b**. Maximum inhibition was observed at the highest concentration of 10 μM which represents a concentration dependent clonogenic growth inhibition. The total colonies were counted by molecular imaging system Vilber Fusion Fx software and the values were represented as a total number of colonies vs. concentration.

### Acridine orange/ethidium bromide (AO/EB) staining

Acridine orange/ethidium bromide (AO/EB) staining assay was carried out to differentiate between live, apoptotic and necrotic cells.<sup>[27]</sup> AO can permeate the intact cell membrane and stain the nuclei green, whereas EB can only stain the nuclei of cells

that have lost membrane integrity, in red. It can be inferred from Figure 6a that the control cells displayed normal morphology and appeared green in colour. Fluorescence microscopic images of MCF-7 cells treated with 10 μM of the compound **5b** clearly showed morphological changes such as cell shrinkage, membrane blebbing, chromatin condensation, and apoptotic body formation, suggesting that it induced apoptosis in MCF-7 cells. On the other hand, it can be observed from Figure 6b, that the control cells showed normal morphology and appeared green in colour, whereas, **14b** has induced morphological changes in the B16F10 cells like membrane blebbing, chromatin condensation, cell shrinkage along with apoptotic body formation at 10 μM concentration after 24 h of incubation. Both of the compounds exhibited these phenomena in a dose dependent manner.

### DAPI nucleic acid staining

DAPI (4',6-diamidino-2-phenylindole) is a fluorescent dye capable of strong binding to the A-T rich sequences of DNA and aids in the visualization of chromatin condensation or nuclear damage. It distinguishes live cells from apoptotic cells by staining the characteristic condensed nuclei of the latter bright blue.<sup>[28]</sup> Therefore, this staining technique was performed to detect the induction of apoptosis by the compounds **5b** and **14b** in MCF-7 and B16F10 cells, respectively. From Figure 7, it was established that the nuclear structure of untreated control cells was intact whereas MCF-7 and B16F10 cells treated with

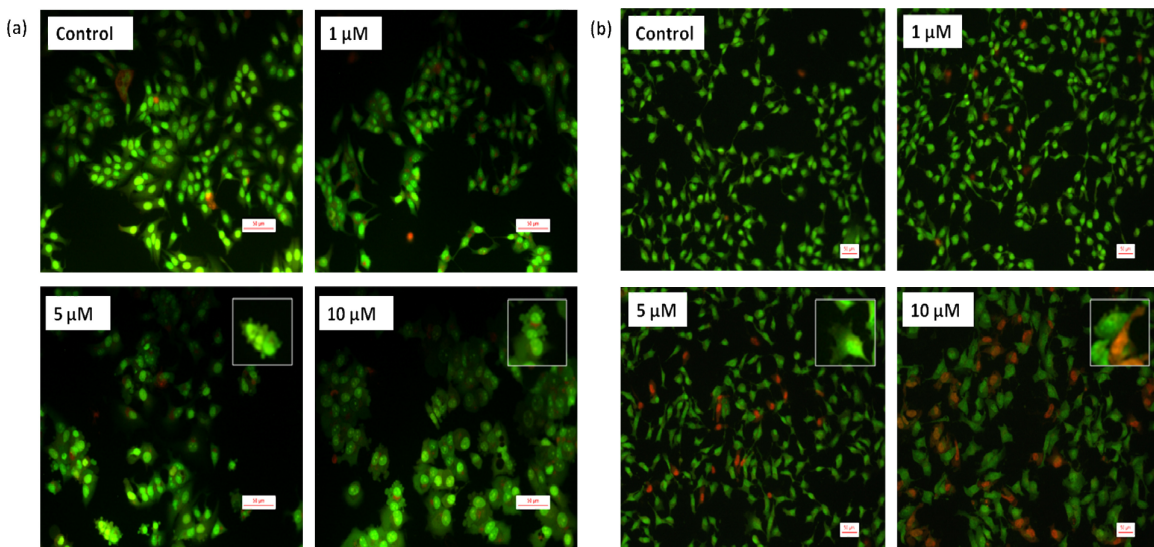


**Figure 6.** (a) AO/EB staining of **5b** in the breast cancer cell line MCF-7. (b) AO/EB staining of **14b** in the melanoma cell line B16F10. Cells were treated with **5b** and **14b** at the concentrations of 1, 5 and 10  $\mu\text{M}$  and compared with control (DMSO treatment).

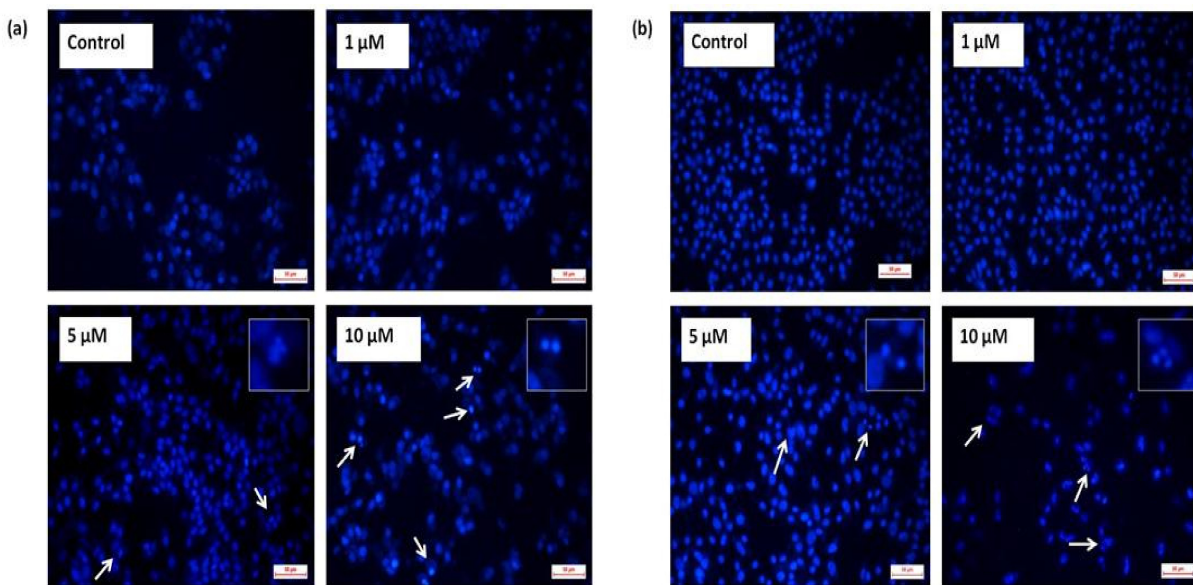


**Figure 7.** Nuclear morphology of cancer cells after DAPI staining. (a) MCF-7 cells were treated with different concentrations of the compound **5b** for 24 h and stained with DAPI. (b) B16F10 cells were treated with different concentrations of the compound **14b** for 24 h and stained with DAPI. The control represents DAPI stain of MCF-7 and B16F10 cells without **5b** and **14b** treatment. The images were captured with a fluorescence microscope at 200x magnification.

**5b** and **14b**, respectively displayed condensed, horse-shoe shaped or fragmented nuclei.

#### Flow-cytometry analysis

Usually, anticancer therapeutics prevent the proliferation of cancer cells by blockade of the cell cycle at a specific checkpoint. From the in vitro screening results, it was evident

that the compounds **5b** and **14b** showed significant activity against the MCF-7 and B16F10 cells, respectively. Hence, it was our interest to figure out whether this cytotoxicity was due to cell cycle arrest, through cell cycle analysis. MCF-7 and B16F10 cells were treated with the compounds **5b** and **14b** respectively, at concentrations of 1, 5 and 10  $\mu\text{M}$  for 24 h, stained with propidium iodide and further analyzed by using BD FACSVer<sup>TM</sup> flow analyzer. The results from Figure 8a indicated that the

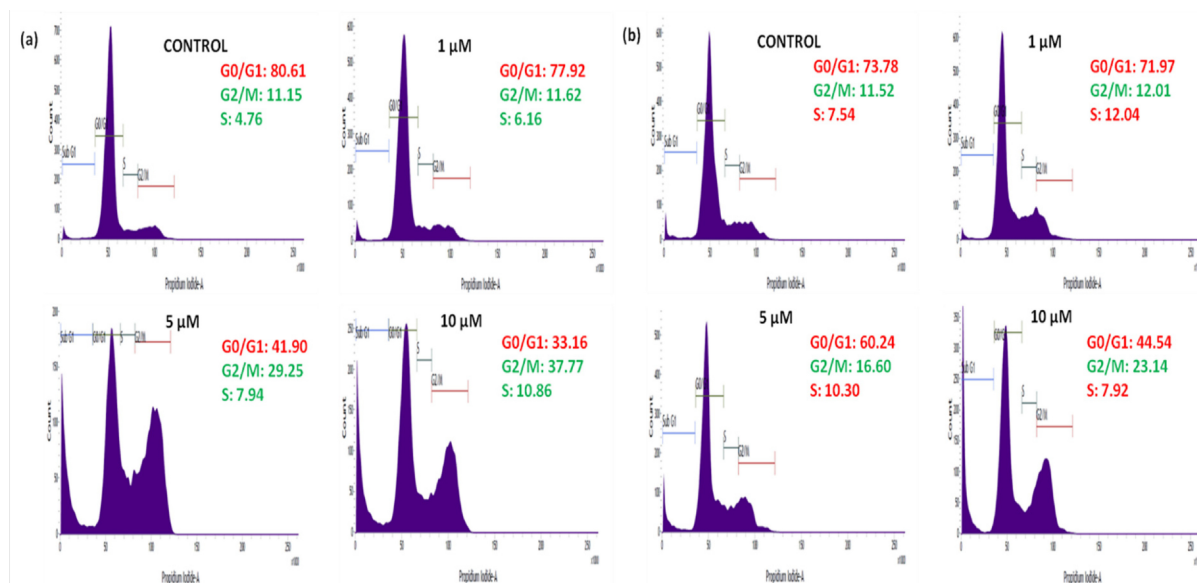


**Figure 8.** Effect of **5b** and **14b** compounds on the cell cycle progression of MCF-7 and B16F10, respectively. (a) MCF-7 cells were treated with compound **5b** and cell cycle analysis was performed after 24 h of incubation by using 1, 5 and 10  $\mu$ M concentrations. (b) B16F10 cells were treated with **14b** and cell cycle analysis was performed. The analysis of cell cycle distribution was performed by using propidium iodide staining method.

MCF-7 untreated control cells exposed to DMSO showed 11.15% cells in G2/M phase, whereas compound **5b** treatment resulted in increased G2/M population to 37.77% in 24 h. Moreover, the percentage of cells in S phase was 6.16, 7.94 and 10.86% with 1, 5 and 10  $\mu$ M of **5b** respectively, in comparison to the control cells where 4.76% phase arrest was observed. These results clearly indicated that treatment of MCF-7 cells with compound **5b** resulted in G2/M and S phase arrest. On the other hand, the results from Figure 8b showed that the control untreated cells of B16F10 showed 11.52% cells in G2/M phase, whereas cells treated with **14b** showed 12.01, 16.60 and 23.14% increase in G2/M population at 1, 5 and 10  $\mu$ M concentrations respectively after 24 h. These results indicated that there was an increased G2/M phase arrest in B16F10 cells treated with **14b**.

#### Relative viscosity experiment

Relative viscosity experiments were performed to assess the nature of the interaction of the most potent cytotoxic compounds **5b** and **14b** with DNA. Intercalation of planar aromatic molecules into DNA leads to a significant increase in the viscosity of DNA solutions by lengthening the double helix; whereas groove binders and DNA surface binders show an only slight increase in viscosity. In contrast, a considerable reduction in the relative viscosity of DNA solutions is exhibited by covalent DNA-binders. The relative changes in viscosity were noted for the DNA solutions upon addition of increasing concentrations of the compounds **5b** and **14b** and plotted graphically in Figure 9. The results obtained were compared with those from the controls, Ethidium Bromide, Hoechst 33258 and Harmine.

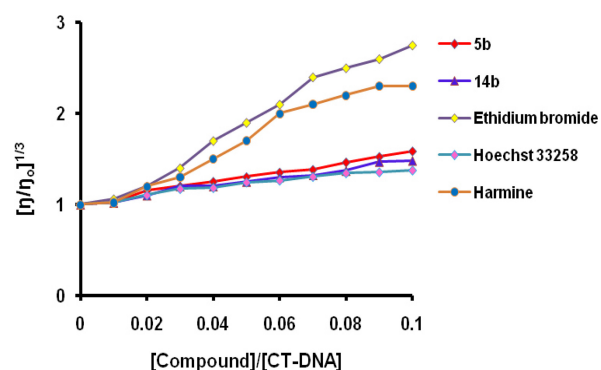


**Figure 9.** Relative viscosity experiment of **5b** and **14b** with CT-DNA. Ethidium Bromide, Harmine and Hoechst 33258 were used as controls.

and Harmine. Ethidium bromide and Harmine, being DNA intercalators, displayed a profound increase in the relative viscosity; whereas only a slight increase was produced by Hoechst 33258, a minor groove binder. Interestingly, there was a slight increase in relative viscosity of the complex solutions upon raising the concentration of **5b** and **14b** gradually, signifying DNA minor groove binding. Moreover, they produced a considerably higher viscosity of DNA solution than that of Hoechst 33258, indicating significant minor groove binding affinity.

#### Molecular modeling

Molecular docking simulations were performed to identify the interaction of structural components of the 1,2,3-triazolo-fused-

tetrahydro- $\beta$ -carboline derivatives with the DNA duplex d(CCGGAATTCGCG)<sub>2</sub>. The docked poses for the compounds **5b** and **14b**, shown in Figure 10, illustrate their non-covalent

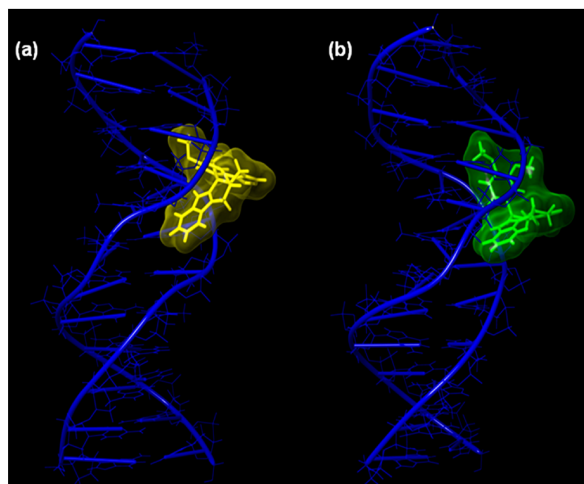


**Figure 10.** Docked poses of (a) **5b** and (b) **14b** in the DNA minor groove.

binding in the curve of the minor groove in the AT-rich region. The binding of the molecules to DNA distorted the helical axis by approximately 4° and also lengthened the minor groove by a few angstroms. In both **5b** and **14b**, the saturated methylene groups adjacent to the piperidine ring make them non-planar to bend them along the minor groove curvature. Additionally, the 1,2,3-triazole moiety participated in side wise  $\pi$ - $\pi$  stacking and hydrogen-bonding with the DNA base pairs. The hydrogen bonds between the indole -NH, methoxy oxygens and the base pairs play a key role in the electronic stabilization of minor groove binding. In the hexaheterocyclic series **5a–r**, the stereochemistry at C-1 does not have much influence on the docking scores; whereas in the pentaheterocyclic series **14a–l**, the *trans*-diastereomers were more efficient in adopting a crescent form to bind along the minor groove curvature.

Further, to study the stability of the DNA-ligand complex, the top scored poses of **5b** and **14b** with DNA were subjected to Molecular Dynamics (MD) simulations for 4 ns. The images of **5b**-DNA complex throughout a 4 ns MD simulation are shown in Figure 11. The plot of root-mean-squared deviation (RMSD) of the atoms of the backbone as a function of time is shown in Figure 12. From the plot, it can be deduced that the compounds did not induce large-scale conformational changes in DNA double helix over the course of 4 ns MD simulation. This can be partly attributed to the van der Waals interactions because the shape of the ligands is appropriate for binding in the DNA minor groove. Generalized Born (GB) method was employed for calculating the binding interaction energies ( $E_{int}$ ) of the ligands with DNA. According to the  $E_{int}$  values in Table 2, it was concluded that **5b** and **14b** are favourable for binding in the minor groove of the DNA with a stable complex formation.

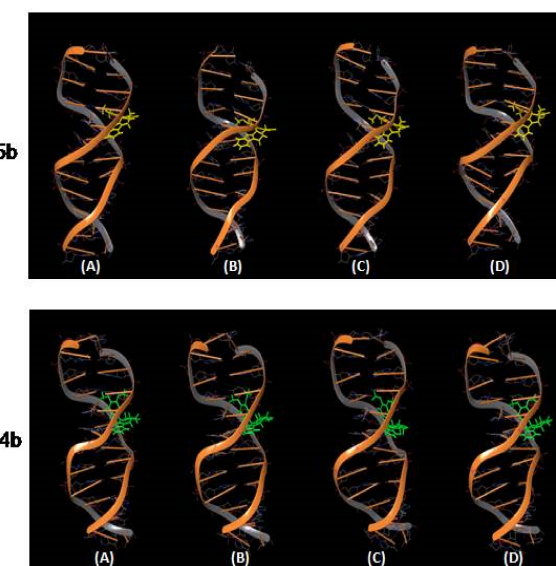


**Figure 11.** Snapshots of DNA-**5b** (top) and DNA-**14b** (bottom) complexes at 0 ns (A), 1 ns (B), 2 ns (C) and 4 ns (D).

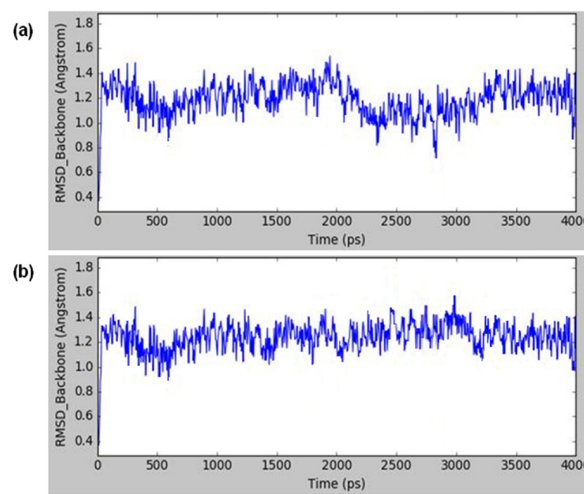


**Figure 12.** RMSD of the trajectories from backbone for (a) **5b** and (b) **14b** versus simulation time (4 ns).

**Table 2.** Energy of interaction ( $E_{int}$ ) calculated by Generalized Born method after 4 ns MD simulation.

Complex	$E_{int}$ (kcal mol <sup>-1</sup> )
DNA- <b>5b</b>	-21.23
DNA- <b>14b</b>	-23.11

### Structure-Activity Relationship (SAR)

The SAR of the novel 1,2,3-triazolo-fused-tetrahydro- $\beta$ -carboline derivatives were derived based on the *in vitro* cytotoxicity and DNA-binding affinity studies. In the hexaheterocyclic series, **5a–r**

r, only the compounds **5a** and **5b** displayed significant cytotoxicity against the cancer cell lines investigated, which inferred that free indole NH is essential for cytotoxicity. On the other hand, the role of indole NH in cytotoxicity can also be affirmed by molecular docking, where it formed hydrogen-bonding with the base pairs of DNA. Some of the remaining N-substituted indole compounds **5c-r** displayed moderate cytotoxicities in the range from 25 to 49  $\mu\text{M}$  in the cell lines investigated while the rest of the compounds were found to be inactive ( $\text{IC}_{50} > 50 \mu\text{M}$ ). Moreover, methoxy substituents on the C1 phenyl ring of **5b** capable of hydrogen-bonding made the compounds more active with better DNA-binding potential, compared to other compounds.

Among the pentaheterocyclic series **14a-l**, compounds with *trans*-configuration possessed significant cytotoxicity and DNA-binding affinity due to their ability to adopt a crescent shape along the curve of the minor groove. SAR studies also revealed that compounds whose C6 phenyl ring is substituted with electron-donating groups such as methyl (**14h**) and methoxy (**14b** and **14d**) displayed better cytotoxicities compared to those with electron-withdrawing groups such as cyano (**14l**), chloro (**14f**) and bromo (**14j**). Thus, the new hybrid polyheterocyclic annulated molecules comprising of two DNA-interactive pharmacophores i.e., a tetrahydro- $\beta$ -carboline system and the annulated triazole moiety amplified the DNA interaction and cytotoxicity through synergism.

## Conclusions

In conclusion, two diverse series of polyheterocyclic annulated 1,2,3-triazolo-fused-tetrahydro- $\beta$ -carboline derivatives have been synthesized by intramolecular azide-alkyne 1,3-dipolar cycloaddition reaction. These compounds have been evaluated for their in vitro cytotoxic activity against selected tumor cell lines and also on normal fibroblasts. Among the hexaheterocyclic series, **5a-r**, the compound **5b** displayed significant cytotoxicity against the MCF-7 cell line with an  $\text{IC}_{50}$  value of  $6.45 \pm 0.37 \mu\text{M}$ ; whereas, among the pentaheterocyclic series, **14a-l**, the derivative **14b** has shown potent cytotoxicity with an  $\text{IC}_{50}$  value of  $4.01 \pm 0.39 \mu\text{M}$  in the B16F10 cell line. Both of these compounds were also found to be safer with lesser cytotoxicity on normal fibroblasts (NRK-49F and HFL-1). Treatment of MCF-7 and B16F10 cells with **5b** and **14b** respectively, resulted in apoptosis, G2/M phase cell cycle arrest, DNA-minor groove binding, inhibition of cell migration and colony formation. Overall, these findings imply that these polyheterocyclics have the potential to be developed as leads and their rational structural modifications may result in promising anticancer agents.

## Supporting Information Summary

Synthetic procedures, biological evaluation experimental details, and spectral information ( $^1\text{H}$  and  $^{13}\text{C}$  spectra) are found in the supporting information of this article.

## Acknowledgements

SN, VP, MV, and RT are thankful to DoP, Ministry of Chemicals & Fertilizers, Govt. of India, for the award of NIPER fellowship. NS gratefully acknowledges SERB, DST, Govt. of India for research grant (YSS-2015-001709).

## Conflict of Interest

The authors declare no conflict of interest.

**Keywords:** antitumor agents • cycloaddition • DNA-minor groove binder • tetrahydro- $\beta$ -carboline • 1,2,3-triazoles

- [1] a) J. J. Marugan, C. Manthey, B. Anaclerio, L. Lafrance, T. Lu, T. Markotan, K. A. Leonard, C. Crysler, S. Eisennagel, M. Dasgupta, B. Tomczuk, *J. Med. Chem.* **2005**, *48*, 926–934; b) M. M. Faul, L. L. Winnroski, C. A. Krumrich, *J. Org. Chem.* **1998**, *63*, 6053–6058; c) M. L. Bennasar, B. Vidal, J. Bosch, *J. Org. Chem.* **1997**, *62*, 3597–3609; d) D. A. Horton, G. T. Bourne, M. L. Smythe, *Chem. Rev.* **2003**, *103*, 893–930; e) H. C. Zhang, H. Ye, A. F. Moretto, K. K. Brumeld, B. E. Maryano, *Org. Lett.* **2000**, *2*, 89–92.
- [2] a) J. L. Sessler, D. -G. Cho, V. Lynch, *J. Am. Chem. Soc.* **2006**, *128*, 16518–16519; b) M. W. Robinson, J. H. Overmeyer, A. M. Young, P. W. Erhardt, W. A. Maltese, *J. Med. Chem.* **2012**, *55*, 1940–1956; c) M. Simoes, R. N. Bennett, E. A. S. Rosa, *Nat. Prod. Rep.* **2009**, *26*, 746–757; d) M. Ishikura, K. Yamada, T. Abe, *Nat. Prod. Rep.* **2010**, *27*, 1630–1680; e) M. Sechi, M. Derudas, R. Dalloccchio, A. Dessi, A. Bacchini, L. Sannia, F. Carta, M. Palomba, O. Ragab, C. Chan, R. Shoemaker, S. Sei, R. Dayam, N. Neamati, *J. Med. Chem.* **2004**, *47*, 5298–5310; f) G. Zhou, D. Wu, B. Snyder, R. G. Ptak, H. Kaur, M. Gochin, *J. Med. Chem.* **2011**, *54*, 7220–7231.
- [3] a) R. A. Abramovitch, I. D. Spencer, *Adv. Heterocycl. Chem.* **1964**, *3*, 79–207; b) J. R. F. Allen, B. R. Holmstedt, *Phytochemistry* **1980**, *19*, 1573.
- [4] a) R. Cao, W. Peng, Z. Wang, A. Xu, *Curr. Med. Chem.* **2007**, *14*, 479–500; b) M. El-Sayed, R. Verpoorte, *Phytochem. Rev.* **2007**, *6*, 277–305; c) F. -E. Chen, J. Huang, *Chem. Rev.* **2005**, *105*, 4671–4706.
- [5] S. Nekkanti, K. Veeramani, S. Sujana Kumari, R. Tokala, N. Shankaraiah, *RSC Adv.* **2016**, *6*, 103556–103566.
- [6] P. R. Jenkins, J. Wilson, D. Emmerson, M. D. Garcia, M. R. Smith, S. J. Gray, R. G. Britton, S. Mahale, B. Chaudhuri, *Bioorg. Med. Chem.* **2008**, *16*, 7728–7739.
- [7] A. H. Abadi, D. A. Abouel-Ella, N. S. Ahmed, B. D. Gary, J. T. Thaiparambil, H. N. Tinsley, A. B. Keeton, G. A. Piazza, *Arzneim. Forsch.* **2009**, *59*, 415–421.
- [8] Y. Fang, Y. Chen, L. Yu, C. Zheng, Y. Qi, Z. Li, Z. Yang, Y. Zhang, T. Shi, J. Luo, M. Liu, *J. Natl. Cancer Inst.* **2013**, *105*, 47–58.
- [9] F. Leteurtre, J. Madalengoitia, A. Orr, T. J. Guzi, E. Lehnert, T. Macdonald, Y. Pommier, *Cancer Res.* **1992**, *52*, 4478–4483.
- [10] a) N. Sunder-Plasmann, V. Sarli, M. Gartner, M. Utz, J. Seiler, S. Huemmer, T. U. Mayer, T. Surrey, A. Giannis, *Bioorg. Med. Chem.* **2005**, *13*, 6094–6111; b) N. Shankaraiah, S. Nekkanti, K. J. Chudasama, K. R. Senwar, P. Sharma, M. K. Jeengar, V. G. M. Naidu, V. Srinivasulu, A. Kamal, *Bioorg. Med. Chem. Lett.* **2014**, *24*, 5413–5417.
- [11] a) K. L. Rinehart, J. Kobayashi, G. C. Harbour, R. G. Hughes Jr., S. A. Miszak, T. A. Scahill, *J. Am. Chem. Soc.* **1984**, *106*, 1524–1526; b) J. Kobayashi, G. C. Harbour, J. Gilmore, K. L. Rinehart Jr., *J. Am. Chem. Soc.* **1984**, *106*, 1526–1528.
- [12] J. Jiang, C. Hu, *Molecules* **2009**, *14*, 1852–1859.
- [13] F. Leteurtre, J. S. Madalengoitia, A. Orr, T. J. Guzi, E. K. Lehnert, T. L. Macdonald, Y. Pommier, *Cancer Res.* **1992**, *52*, 4478–4483.
- [14] a) Y. -C. Shen, Y. -T. Chang, C. -L. Lin, C. -C. Liaw, Y. H. Kuo, L. -C. Tu, S. F. Yeh, J. -W. Chern, *Mar. Drugs* **2011**, *9*, 256–277; b) L. S. Santos, C. Theoduloz, R. A. Pilli, J. Rodriguez, *Eur. J. Med. Chem.* **2009**, *44*, 3810–3815; c) R. Kumar, L. Gupta, P. Pal, S. Khan, N. Singh, S. B. Katiyar, S. Meena, J. Sarkar, S. Sinha, J. K. Kanaujiya, S. Lochab, A. K. Trivedi, P. M. S. Chauhan, *Eur. J. Med. Chem.* **2010**, *45*, 2265–2276; d) R. Skouta, M. Hayano, K. Shimada, B. R. Stockwell, *Bioorg. Med. Chem. Lett.* **2012**, *22*, 5707–5713; e) Y. Zeng, Y. Zhang, Q. Weng, M. Hu, G. Zhong, *Molecules*

- 2010, 15, 7775–7791; f) C. Zheng, Y. Fang, W. Tong, G. Li, H. Wu, W. Zhou, Q. Lin, F. Yang, Z. Yang, P. Wang, Y. Peng, X. Pang, Z. Yi, J. Luo, M. Liu, Y. Chen, *J. Med. Chem.* 2014, 57, 600–612; g) G. Dong, S. Wang, Z. Miao, J. Yao, Y. Zhang, Z. Guo, W. Zhang, C. Sheng, *J. Med. Chem.* 2012, 55, 7593–7613.
- [15] D. K. Dalvie, A. S. Kalgutkar, S. C. Khojasteh-Bakht, R. S. Obach, J. P. O' Donnell, *Chem. Res. Toxicol.* 2002, 15, 269–299.
- [16] W. S. Horne, M. K. Yadav, C. D. Stout, M. R. Ghadiri, *J. Am. Chem. Soc.* 2004, 126, 15366–15367.
- [17] a) H. C. Kolb, K. B. Sharpless, *Drug Discov. Today* 2003, 8, 1128–1137; b) V. D. Bock, H. Hiemstra, J. H. van Maarseveen, *Eur. J. Org. Chem.* 2006, 51–68; c) M. Meldal, C. W. Tornøe, *Chem. Rev.* 2008, 108, 2952–3015; d) F. Amblard, J. H. Cho, R. F. Schinazi, *Chem. Rev.* 2009, 109, 4207–4220; e) A. Qin, J. W. Y. Lam, B. Z. Tang, *Chem. Soc. Rev.* 2010, 39, 2522–2544.
- [18] a) V. Sai Sudhir, R. B. Nasir Baig, S. Chandrasekaran, *Eur. J. Org. Chem.* 2008, 2423–2429; b) R. A. Turner, A. G. Oliver, R. Scott Lokey, *Org. Lett.* 2007, 9, 5011–5014; c) F. Couty, F. Durrat, D. Prim, *Tetrahedron Lett.* 2004, 45, 3725–3728; d) I. Akritopoulou-Zanze, V. Gracias, S. W. Djuric, *Tetrahedron Lett.* 2004, 45, 8439–8441.
- [19] P. G. Baraldi, M. A. Tabrizi, D. Preti, F. Fruttarolo, B. Avitabile, A. Bovero, G. Pavani, M. Carmen Nunez del Carretero, R. Romagnoli, *Pure Appl. Chem.* 2003, 75, 187–194.
- [20] K. Uytterhoeven, J. Sponer, L. Van Meervelt, *Eur. J. Biochem.* 2002, 269, 2868–2877.
- [21] M. D'Incalci, N. Badri, C. M. Galmarini, P. Allavena, *Br. J. Cancer* 2014, 111, 646–650.
- [22] a) W. A. Silva, M. T. Rodrigues, N. Shankaraiah, R. B. Ferreira, C. K. Z. Andrade, R. A. Pilli, L. S. Santos, *Org. Lett.* 2009, 11, 3238–3241; b) N. Shankaraiah, K. P. Siraj, S. Nekkanti, V. Srinivasulu, M. Satish, P. Sharma, K. R. Senwar, M. V. P. S. Vishnuvardhan, S. Ramakrishna, A. Kamal, *Bioorg. Chem.* 2015, 59, 130–139; c) A. Kamal, V. Srinivasulu, V. L. Nayak, M. Sathish, N. Shankaraiah, C. Bagul, N. V. S. Reddy, N. Rangaraj, N. Nagesh, *ChemMedChem* 2014, 9, 2084–2098; d) S. Nekkanti, N. Praveen Kumar, P. Sharma, A. Kamal, F. M. Nachigall, O. Forero-Doria, L. S. Santos, N. Shankaraiah, *RSC Adv.* 2016, 6, 2671–2677; e) N. Shankaraiah, C. Jadala, S. Nekkanti, K. R. Senwar, N. Nagesh, S. Shrivastava, V. G. M. Naidu, M. Sathish, A. Kamal, *Bioorg. Chem.* 2016, 64, 42–50; f) S. Nekkanti, K. Veeramani, N. Praveen Kumar, N. Shankaraiah, *Green Chem.* 2016, 18, 3439–3447.
- [23] B. J. Stokes, S. Liu, T. G. Driver, *J. Am. Chem. Soc.* 2011, 133, 4702–4705.
- [24] F. Ungemach, D. Soerens, R. Weber, M. DiPietro, O. Campos, P. Mokry, J. M. Cook, J. V. Silverton, *J. Am. Chem. Soc.* 1980, 102, 6976–6984 (Also see the supporting information).
- [25] P. Friedl, K. Wolf, *Nat. Rev. Cancer* 2003, 3, 362–374.
- [26] N. A. Franken, H. M. Rodermond, J. Stap, J. Haveman, C. van Bree, *Nat. Protoc.* 2006, 1, 2315–2319.
- [27] K. Liu, P. Liu, R. Liu, X. Wu, *Med. Sci. Monit. Basic Res.* 2015, 21, 15–20.
- [28] B. Chazotte, *Cold Spring Harb Protoc.* 2011(2011):pdb.prot5556.

Submitted: March 23, 2017

Revised: July 24, 2017

Accepted: July 31, 2017